Alterations in Cerebral Metabolic Rate and Blood Supply across the Adult Lifespan

Hanzhang Lu[1], Feng Xu[1], Karen M. Rodrigue[2], Kristen M. Kennedy[2], Yamei Cheng[1], Blair Flicker[2], Andrew C. Hebrank[2], Jinsoo Uh[1] and Denise C. Park[2]

[1]Advanced Imaging Research Center, University of Texas Southwestern Medical Center, Dallas, TX 75390, USA and [2]Center for Vital Longevity, School of Behavioral and Brain Sciences, University of Texas at Dallas, Dallas, TX 75235, USA

Address correspondence to Dr Hanzhang Lu, Advanced Imaging Research Center, University of Texas Southwestern Medical Center, 5323 Harry Hines Boulevard, Dallas, TX 75390, USA. Email: hanzhang.lu@utsouthwestern.edu.

With age, the brain undergoes comprehensive changes in its function and physiology. Cerebral metabolism and blood supply are among the key physiologic processes supporting the daily function of the brain and may play an important role in age-related cognitive decline. Using MRI, it is now possible to make quantitative assessment of these parameters in a noninvasive manner. In the present study, we concurrently measured cerebral metabolic rate of oxygen ($CMRO_2$), cerebral blood flow (CBF), and venous blood oxygenation in a well-characterized healthy adult cohort from 20 to 89 years old (N = 232). Our data showed that $CMRO_2$ increased significantly with age, while CBF decreased with age. This combination of higher demand and diminished supply resulted in a reduction of venous blood oxygenation with age. Regional CBF was also determined, and it was found that the spatial pattern of CBF decline was heterogeneous across the brain with prefrontal cortex, insular cortex, and caudate being the most affected regions. Aside from the resting state parameters, the blood vessels' ability to dilate, measured by cerebrovascular reactivity to 5% CO_2 inhalation, was assessed and was reduced with age, the extent of which was more prominent than that of the resting state CBF.

Keywords: aging, blood oxygenation, cerebral blood flow, cerebral metabolism, cerebrovascular reactivity, MRI

Introduction

Extensive literature has established that cognitive function declines with age, even in healthy adults (Craik 1983; Hasher and Zacks 1988; Salthouse et al. 1989; Park et al. 1996; Salthouse 1996; Cepeda et al. 2001; Park et al. 2002). The neurobiological basis of these changes has also been partially elucidated and includes structural shrinkage (Raz et al. 2005; Salat et al. 2004; Raz and Kennedy 2009), the development of white matter lesions (Ross et al. 2005; Bohnen et al. 2009), and altered neuronal function (Rypma and D'Esposito 2000; Gutchess et al. 2005; Andrews-Hanna et al. 2007). Another plausible contribution to age-related cognitive decline is alterations in cerebral metabolism and blood supply (Iadecola et al. 2009), especially considering the increased risk of arterial stenosis, hypertension, and stroke with aging. The present study aims to investigate age-related alterations in these physiologic processes.

The human brain represents about 2% of the total body weight but consumes about 20% of the total energy (Attwell and Laughlin 2001). The energy homeostasis of the brain can be characterized by 3 physiologic parameters: venous oxygenation level (Y_v), cerebral blood flow (CBF), and cerebral metabolic rate of oxygen ($CMRO_2$) (Kety and Schmidt 1948) (for a diagram illustration, see Fig. 1). Arterial vessels deliver blood that has an oxygenation level close to unity, the flow rate of which is denoted by CBF. When the blood transits through capillary beds, a portion of the carried oxygen is extracted by brain tissue for its metabolism, the rate of which is denoted by $CMRO_2$. The portion that remains in the blood will determine the venous oxygenation, Y_v, and is drained through veins. A conceptual simplification of this system is that CBF and $CMRO_2$ reflect oxygen supply and demand, respectively, and Y_v signifies the remaining fraction after demand has been met from the available supply. The present study will assess how the homeostasis among these 3 variables may alter with age.

Aside from the static parameters described above, we will also measure a dynamic parameter called cerebrovascular reactivity (CVR), which has important implications for the interpretation of functional MRI (fMRI) data in aging (D'Esposito et al. 2003). Recently, there has been a great deal of evidence from the functional imaging literature indicating that older adults show different activation signals relative to young adults when performing cognitive tasks (Rypma and D'Esposito 2000; Gutchess et al. 2005; Duverne et al. 2009; Park and Reuter-Lorenz 2009). One issue that clouds interpretation of this observation is that the fMRI signal relies upon an indirect vascular response to detect neural activation (Ogawa et al. 1992; Iadecola 2004). It is likely that age differences in CVR affect blood flow responses, which modulates the fMRI signal independent of neural activity. Thus, cognitive neuroscience of aging research will be tremendously advanced by the characterization of the age-related changes in CVR.

In the present study, we conducted an investigation on age-related alterations in cerebral metabolic and vascular parameters in a well-characterized healthy adult cohort from 20 to 89 years old. We measured Y_v, CBF, and $CMRO_2$ of each participant under resting conditions. We also employed inhalation of 5% CO_2 gas mixture to measure CVR on a region-specific basis.

Materials and Methods

Participants

Participants were recruited from the cohort of a large-scale aging study, the Dallas Lifespan Brain Study (DLBS), which is a comprehensive life span study on cognitive function and neuroimaging. DLBS includes detailed and comprehensive measures of brain structure and function using MRI, as well as multiple measurements of a broad range of behavioral measures of cognitive function. The Health Insurance Portability and Accountability Act (HIPAA) compliant protocol was approved by the UT Southwestern Institutional Review Board and written informed consent was obtained from all participants. All participants underwent extensive health screening and had no contraindications to MRI scanning (pacemaker, implanted metallic objects, and claustrophobia) and were generally of good health, with no serious or unstable medical conditions such as neurological disease, brain injury, uncontrollable shaking, past bypass surgery or chemotherapy, or use of medications that affect cognitive function. All participants were

highly right-handed native English speakers with at least a high school education and a Mini-Mental State Exam (MMSE) (Folstein et al. 1975) score of 26 or greater. The racial and ethnic distribution of the sample included American Indian (2 or 1%), Asian American (9 or 4%), African American (12 or 5%), Hispanic (10 or 4%), Multiracial (4 or 2%), and Caucasian (195 or 84%). Thirty-three subjects who reported a diagnosis of hypertension were taking antihypertensive medications (mostly angiotensin converting enzyme inhibitors, beta-blockers, and angiotensin II receptor antagonists). The hypertensive participants were significantly older than their normotensive peers, $t = -8.59$, $P < 0.001$, but did not differ on education, $t = -0.491$, ns, or MMSE, $t = 1.22$, ns. Mean systolic and diastolic blood pressure for the hypertensive group (137.85/83.48 mm Hg) significantly exceeded (for systolic pressure, $t = 5.10$, $P < 0.001$; for diastolic pressure, $t = 2.70$, $P = 0.009$) that of the controls (122.73/79.35 mm Hg).

Global venous oxygenation, CBF, and $CMRO_2$ were measured in a total of 232 subjects (aged 20–89). Regional CBF was also measured in these subjects. However, data were not usable in a few subjects due to pulse sequence problems, thus regional CBF data were available in 226 subjects. We also offered the CVR option to all subjects, but some participants declined this scan because of concerns about CO_2 breathing. Therefore, a subset of 152 subjects participated in the CVR scan. We note, however, that the breathing paradigm used in our study was actually easily tolerable and all subjects who agreed to do the CO_2 study completed the scan without problem. Table 1 lists demographic information for the participants.

Overview of Experimental Procedures

MRI investigations were performed on a 3 T MR system (Philips Medical System). A body coil was used for radio frequency transmission and an 8-channel head coil with parallel imaging capability was used for signal reception. Foam padding was used to stabilize the head to minimize motion. The cerebral metabolic and vascular measurements described below were completely noninvasive and conducted in a scan session of approximately 30 min.
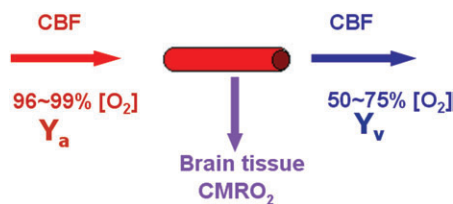

Figure 1. Diagram illustrating the homeostasis of oxygen delivery and consumption in the brain. Arterial (Y_a) and venous (Y_v) oxygenation levels are the percentage of hemoglobin in the blood that is bound to oxygen. Y_a is close to unity and, relative to Y_v, does not vary much across individuals. Arterial vessels deliver blood to brain tissue, the flow rate of which is denoted by CBF. When the blood transits through capillary beds, a portion of the carried oxygen is extracted by brain tissue for its metabolism, the rate of which is denoted by $CMRO_2$. The portion that remains in the blood will determine the value of Y_v and is drained through veins.

Global Venous Oxygenation

Global venous oxygenation, Y_v, was measured noninvasively from superior sagittal sinus (SS) using a recently developed technique T_2-relaxation-under–spin-tagging (TRUST) MRI (Lu and Ge 2008). The imaging parameters were voxel size $3.44 \times 3.44 \times 5$ mm³, time repetition (TR) = 8000 ms, time to inversion (TI) = 1200 ms, 4 time echos (TEs): 0, 40, 80, and 160 ms, and duration 4.3 min.

The data processing procedures for TRUST MRI were based on an algorithm described previously (Lu and Ge 2008). Briefly, after pairwise subtraction between control and tag images, a preliminary region of interest (ROI) was manually drawn to include the SS. This ROI tended to have about 30–50 voxels, which include the vein as well as some surrounding tissue. To further define the venous voxels, the voxels with highest blood signals (according to the difference signals) in the ROI were chosen as the final mask for spatial averaging. For the purpose of standardizing protocol, we use 4 peak voxels in this study, although we have tested the effect of voxel number and found that the results are relatively insensitive to the voxel number (Lu and Ge 2008). The venous blood signals were fitted to a monoexponential function to obtain T_2. The T_2 was in turn converted to Y_v via a calibration plot obtained by in vitro blood experiments under controlled oxygenation, temperature, and hematocrit conditions (Lu et al. 2004; Zhao et al. 2007; Lu and Ge 2008).

Global CBF

Total CBF to the entire brain was measured with phase-contrast (PC) flow velocity MRI with imaging slices positioned at a level that allowed simultaneous assessment of the 4 feeding arteries, including left/right internal carotid and left/right vertebral arteries (Aslan et al. 2010). To visualize these arteries and to ensure correct positioning of PC MRI, a time-of-flight angiogram was first acquired with the following acquisition parameters: TR/TE/flip angle = 23 ms/3.45 ms/18°, field of view (FOV) = $160 \times 70 \times 160$ mm³, voxel size $1.0 \times 1.0 \times 1.5$ mm³, number of slices = 47, one saturation slab of 60 mm positioned above the imaging slab, and duration 1 min 26 s. The PC MRI was then performed with the following parameters: single slice, voxel size = $0.45 \times 0.45 \times 5$ mm³, FOV = $230 \times 230 \times 5$ mm³, TR/TE = 20/7 ms, flip angle = 15°, maximum velocity encoding = 80 cm/s, and duration 30 s.

To quantify total CBF from PC MRI data, left/right internal carotid and left/right vertebral arteries were identified from the phase image (i.e., velocity map). These arteries were distinguishable from the veins (e.g., internal jugular veins) because their blood flow direction is opposite to that of the veins. An ROI was then drawn on each of the 4 arteries based on the magnitude image (Aslan et al. 2010). The ROI mask was applied to the velocity map and the integration of the map (i.e., velocity × area) yielded CBF in units of milliliters per minute. We have tested the interrater variability of this processing procedure and found that the results are highly consistent across raters, $r > 0.99$ (Supplementary Fig. S1).

To account for brain size differences and to obtain unit mass CBF values, the total CBF was divided by the brain mass obtained from a high-resolution T_1-weighted scan with the following parameters: magnetization-prepared rapid acquisition of gradient echo sequence, TR/TE/TI = 8.1 ms/3.7 ms/1100 ms, flip angle = 18°, voxel size $1 \times 1 \times 1$ mm³, number of slices 160, sagittal slice orientation, and duration 3 min

Table 1

Subject demographic information and number of subjects for each physiologic measure

Age range	20s	30s	40s	50s	60s	70s	80s
Total number of subjects recruited	40	22	33	35	40	40	22
Gender (female/male)	27/13	13/9	23/10	23/12	25/15	23/17	11/11
Education (years, mean ± standard deviation)	16.10 ± 2.39	17.27 ± 2.37	16.27 ± 2.79	17.46 ± 2.44	16.70 ± 2.52	16.10 ± 2.88	16.45 ± 2.48
MMSE (mean ± standard deviation)	28.50 ± 1.26	28.48 ± 1.36	28.57 ± 1.20	28.13 ± 1.15	27.70 ± 1.24	27.14 ± 1.40	27.14 ± 1.17
Number of hypertensive subjects	0	0	1	4	11	8	9
Number of subjects for global venous oxygenation (Y_v)	40	22	33	35	40	40	22
Number of subjects for global CBF	40	22	33	35	40	40	22
Number of subjects for global $CMRO_2$	40	22	33	35	40	40	22
Number of subjects for regional CBF	38	22	31	35	39	40	21
Number of subjects for regional CVR	33	15	22	26	22	24	10

and 57 s. The delineation of brain boundary used the software FSL (FMRIB Software Library, Oxford University, UK). The brain volume was converted to brain mass by assuming a density of 1.06 g/ml (Herscovitch and Raichle 1985). The resulting global CBF value is in units of milliliters per 100 g per minute.

Global CMRO$_2$

Global CMRO$_2$ in units of micromoles per minute was calculated from the Y_v and CBF measures using the Fick principle (Kety and Schmidt 1948):

$$CMRO_2 = CBF \cdot (Y_a - Y_v) \cdot C_a \qquad [1]$$

where C_a is the amount of oxygen molecules that a unit volume of blood can carry, assumed to be 833.7 μmol O_2/100 ml blood based on physiology literature (Guyton and Hall 2005). The arterial oxygenation, Y_a, is close to unity and has been reported to be minimally affected by age (Leenders et al. 1990; Li et al. 2006). To confirm this notion, we measured Y_a using a pulse oximeter in a subset of the subjects (in the ones that participated in the CO_2 study, $N = 152$) and found that the dependence of Y_a on age can be written as $Y_a = 99.06 - 0.02\% \times age$ (see Supplementary Fig. S2), that is, Y_a decreases by 1% every 50 years. Thus, Y_a indeed shows a minimal effect of age. In our CMRO$_2$ calculation, we used the above expression to estimate Y_a of each individual based on his or her age.

Regional CBF

Regional CBF at resting state was measured using arterial spin labeling (ASL) MRI (Garcia et al. 2005; Wong 2007; Wu et al. 2007; Dai et al. 2008). Scan parameters were FOV = 240 × 240 mm^2, matrix = 80 × 80, 27 axial slices, thickness = 5 mm, TR/TE = 4020 ms/14ms, pseudo-continuous labeling with a duration of 1.6 s, delay = 1.5 s, single-shot echo-planar imaging (EPI), 30 pairs of label and control images, and duration 4 min.

ASL MR images were used to calculate a relative CBF map by subtraction of the control and label image sets following procedures established previously (Aslan et al. 2010). The 30 repeated scans were averaged to improve signal-to-noise ratio. We note that the ASL data and the PC MRI data described earlier are complementary, in that PC MRI provides a quantitative estimation of absolute CBF without spatial information, whereas ASL MRI provides a spatially resolved map, but it is a relative measure. We have recently devised a method to combine these 2 images to yield quantitative CBF measures on a region-specific basis (Aslan et al. 2010). This method was used in the present study to determine regional CBF in units of milliliters per 100 g per minute.

Regional CVR

Regional CVR measurement followed protocols established in our previous studies (Yezhuvath et al. 2009). CVR was assessed using hypercapnia induced by 5% CO_2-breathing (mixed with 21% O_2 and 74% N_2). Hypercapnia was administered via a plastic bag with a valve to switch between room air and CO_2 air. A mouthpiece and nose clip were used to achieve mouth-only breathing. A research assistant was inside the magnet room throughout the experiment to switch the valve and monitor the subject. Physiologic parameters, including end-tidal (Et) CO_2, breathing rate, heart rate, and arterial oxygenation (Y_a), were recorded during the experiment (MEDRAD; Novametrix Medical Systems). The type of air breathed in was switched every minute in a manner similar to a block design fMRI experiment, while blood oxygenation level–dependent (BOLD) MR images were acquired for 7 min. Our previous study suggested that CVR measured with 1-min CO2 inhalation is comparable with that with a longer duration (e.g., 4 min) (Yezhuvath et al. 2009), and our experience is that 1-min inhalation is much easier to tolerate. Other imaging parameters were FOV = 220 × 220 mm^2, matrix size = 64 × 64, 43 axial slices, thickness = 3.5 mm, no gap, TR/TE/flip angle = 2000 ms/25ms/80°, single-shot EPI, and duration 7 min.

CVR data were processed using a general linear model (SPM2, University College London, UK) similar to a typical fMRI scan, except that the regressor was the EtCO$_2$ time course rather than the fMRI paradigm. In-house MATLAB (Mathworks) scripts were used to obtain EtCO2 time courses that were synchronized with MRI acquisitions.

Since the hypercapnia-induced vasodilatation is mediated by CO_2 level changes, EtCO$_2$ time course provides an input function to the vascular system. The BOLD time course is the output signal, and by comparing the input and output signals, the vascular system property was determined (Yezhuvath et al. 2009). Absolute CVR is in units of %BOLD signal change per mmHg of EtCO$_2$ change (%BOLD/mmHg CO_2).

Data Analysis

For the global measures of venous oxygenation, CBF, and CMRO$_2$, a multiple regression analysis was employed with the metabolic/vascular measure as the dependent variable. Age and gender were used as the independent variables. As an exploratory analysis, a quadratic age term, that is, age^2, was also added to the model to assess whether a nonlinear equation could yield better fitting of the data. Decade-by-decade time courses were obtained by averaging the subjects in each decade (e.g., 20–29, 30–39, etc.).

For the regional measures, CBF and CVR maps in individual space were processed with Statistical Parametric Mapping (SPM2, University College London, UK) and Hierarchical Attribute Matching Mechanism for Elastic Registration (HAMMER, University of Pennsylvania, PA) software packages. The maps were normalized to the Montreal Neurological Institute (MNI) template space using the high-resolution T_1-weighted image as an intermediate step. We used the HAMMER algorithm for the spatial normalization process because it was shown to be relatively robust even in the presence of brain atrophy, and it also has the option to conduct concentration-preserving transformation (Shen and Davatzikos 2002). This was important to make sure the comparison truly reflected vascular parameters rather than being affected by brain volume reduction. The images were further smoothed using a Gaussian filter with full-width-half-maximum of 12 mm. This step was necessary to account for small differences in gyri/sulci locations across subjects (Ashburner and Friston 2000).

For voxel-by-voxel statistical analysis of CBF and CVR maps, we conducted a multiple regression analysis with age, gender, gray matter probability, and CSF probability as the regressors. The gray and CSF probability indices were obtained by segmentation routines in SPM2. They were included in the model to eliminate any residual partial volume effect at the intravoxel level so that the observed age dependence is not due to an increased CSF fraction or reduced gray matter fraction in older subjects. We note that the white matter probability was not included in the model because it has a fixed relationship with the other 2 probability values, $P_{WM} + P_{GM} + P_{CSF} = 1$, thus its effect is already included in the model. Student t-tests were conducted to identify significant clusters using criteria established in the literature ($P < 0.005$, cluster size = 200 voxels) (Xu et al. 2007). We also performed an ROI analysis on the CBF and CVR images given that ROI methods may provide more valid results than voxel-wise methods alone (Kennedy et al. 2009). ROIs corresponding to major brain regions were automatically determined using the preparcellated MNI brain template (Tzourio-Mazoyer et al. 2002). Eight ROIs were investigated: frontal lobe, parietal lobe, temporal lobe, occipital lobe, insular cortex, limbic regions, sensorimotor regions, and subcortical gray matter. The parameter values within the ROI were averaged. To account for partial volume effect, the ROI value was corrected for gray/white matter probability following procedures used previously (Johnson et al. 2005). A regression analysis was conducted and a multicomparison-corrected P value of 0.05 or less was considered significant.

Results

Global Venous Oxygenation Decreases with Age

Figure 2 shows the scatter plot between Y_v and age ($N = 232$). Regression analysis revealed that age has a statistically significant ($P < 0.0001$) effect on Y_v. Specifically, average Y_v in typical 20-year-old subjects is approximately 64.2%, and it decreases with age at a rate of 1.4% per decade, suggesting that the balance between oxygen demand and supply is gradually
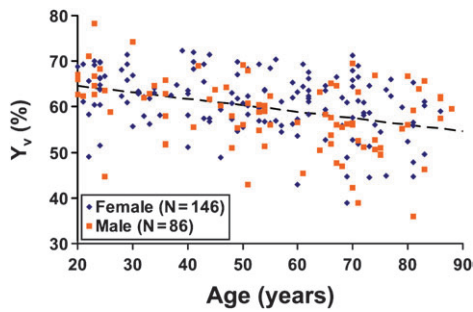
Figure 2. Scatter plot between global venous oxygenation (Y_v) and age (total $N = 232$). Each dot represents data from one subject. The data from women and men are shown with different symbols. The dashed line is a linear fitting of the experimental data from both sexes. Regression analysis showed that age has a significant effect on Y_v ($P < 0.0001$), but a quadratic model did not improve the fitting. Women showed higher Y_v compared with men ($P = 0.0205$).

Figure 3. Global CBF alterations with age. (*a*) Illustration of the imaging slice (yellow) with regards to the major feeding arteries. (*b*) Scatter plot between global CBF and age (total $N = 232$). The data from women and men are shown with different symbols. The dashed line is a linear fitting of the experimental data from both sexes. Regression analysis showed that age has a significant effect on CBF ($P = 0.0065$). Women showed higher CBF compared with men ($P < 0.0001$).

altered with age. A quadratic model with age^2 as an additional regressor did not improve the fit.

Intersubject variability in Y_v was also assessed on a decade-by-decade basis, and it showed a significant increase with age (cross-correlation coefficient between decade and standard deviation of Y_v within the decade $R = 0.81$, $P = 0.0272$). That is, with age, Y_v not only shows a gradual decrease but the intersubject heterogeneity also becomes greater.

Global CBF Decreases with Age

Figure 3*a* illustrates the location of the 4 feeding arteries, from which global CBF was measured. Figure 3*b* shows the scatter plot between CBF and age ($N = 232$). Regression analysis revealed an age-related decrease ($P = 0.0065$) of global CBF at a rate of 0.8 ml/100 g/min per decade, from an average CBF of 58.1 ml/100 g/min in typical 20-year-old subjects.

Global CMRO$_2$ Increases with Age

Figure 4 shows the scatter plot between CMRO$_2$ and age ($N = 232$). Regression analysis revealed that there is paradoxical increase of CMRO$_2$ with age ($P = 0.0101$). Average CMRO$_2$ of typical 20-year-old subjects is approximately 164.1 µmol/100 g/min, and it increases with age at a rate of 2.6 µmol/100 g/min per decade. Therefore, the aging brain appears to suffer from double insults of decreased oxygen supply and increased oxygen demand, resulting in an age-related decrease in venous oxygenation. Note that the CMRO$_2$ value reported in our study is for unit mass brain parenchyma, thus the brain atrophy effect has been accounted for. As far as the total brain oxygen consumption is concerned, an age-related decrease was observed because the brain size is smaller in older subjects (see Discussion for more details).

Regional Specificity of Age-Related CBF Alterations

Figure 5 shows averaged CBF maps for each decade. Visual inspection suggested that age-related CBF decline is heterogeneous across brain regions. Figure 6*a,b* shows the voxels that revealed a significant age-related decrease using voxel-based linear regression ($N = 226$). These regions were found to be prefrontal cortex (including anterior cingulate cortex), insular cortex, and caudate nucleus. All regions were located in the rostral half of the brain. There also appears to be a hemispheric asymmetry in the prefrontal region with the right brain showing more pronounced CBF decline. ROI analysis revealed
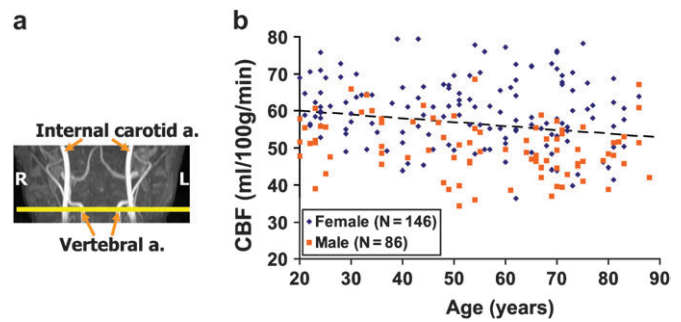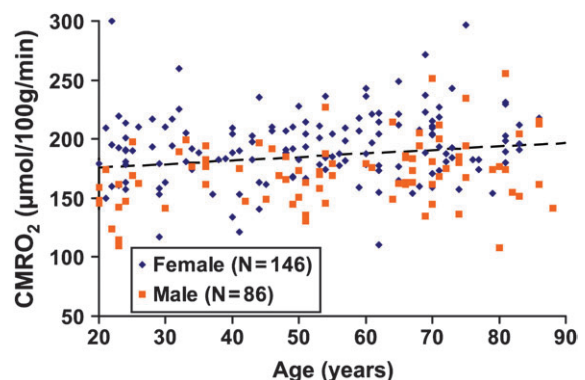

Figure 4. Scatter plot between global CMRO$_2$ and age (total $N = 232$). The data from women and men are shown with different symbols. The dashed line is a linear fitting of the experimental data. Regression analysis showed that age has a positive effect on CMRO$_2$ ($P = 0.0101$). Women showed higher CMRO2 compared with men ($P < 0.0001$).
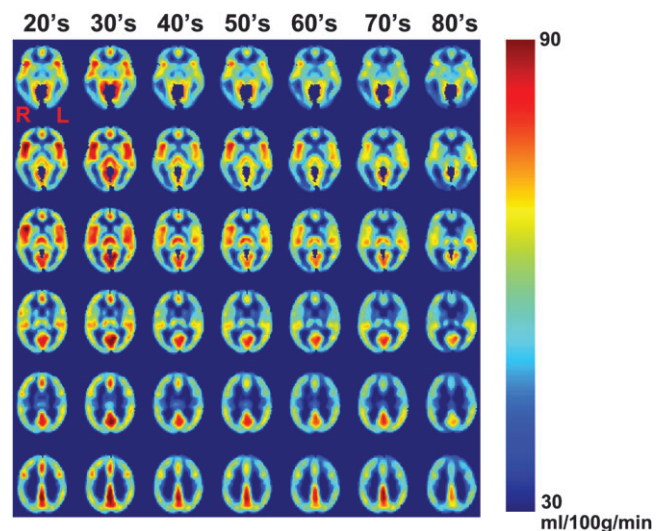

Figure 5. Regional CBF maps as a function of age. Subjects from each decade were grouped, and their CBF maps were averaged for display. Six representative brain sections are shown.

similar findings. Of the 8 major regions assessed, frontal lobe (corrected $P = 0.002$), insula cortex ($P < 0.001$), and subcortical gray matter ($P = 0.016$) showed significant age-related decline.

An age-related CBF increase was also observed in bilateral white matter regions of frontal and parietal lobes (Supplementary Fig. S3). The physiologic mechanism underlying this observation is not clear.

The gender-related CBF difference does not seem to be region specific. Female subjects had higher CBF than male subjects throughout the entire brain (Supplementary Fig. S4).

CVR Decreases with Age

Figure 7 shows the voxels that revealed a significant CVR decrease with age using voxel-based linear regression ($N = 152$). It can be seen that CVR reduction is more prevalent compared with CBF. ROI analysis revealed highly significant age effects in all regions assessed, including frontal lobe (corrected $P < 0.001$), parietal lobe ($P < 0.001$), temporal lobe ($P = 0.003$), occipital lobe ($P = 0.002$), insular cortex ($P < 0.001$), limbic regions ($P < 0.001$), sensorimotor regions ($P < 0.001$), and subcortical gray matter ($P = 0.003$). We have also tested whether a quadratic model can yield a better fit. A trend of improvement was observed in a few regions including the occipital lobe (uncorrected $P = 0.029$), insular cortex ($P = 0.010$), and subcortical gray matter ($P = 0.007$), suggesting that CVR decline may be nonlinear (accelerated) with age.

Decade-by-decade alterations in regional CBF and CVR were also investigated. Since prefrontal cortex showed a significant decline in both CBF and CVR and it is one of the most affected regions in aging (Raz and Kennedy 2009), we have focused on this region using an anatomically defined mask in the literature (Tzourio-Mazoyer et al. 2002). Figure 8 shows the time courses
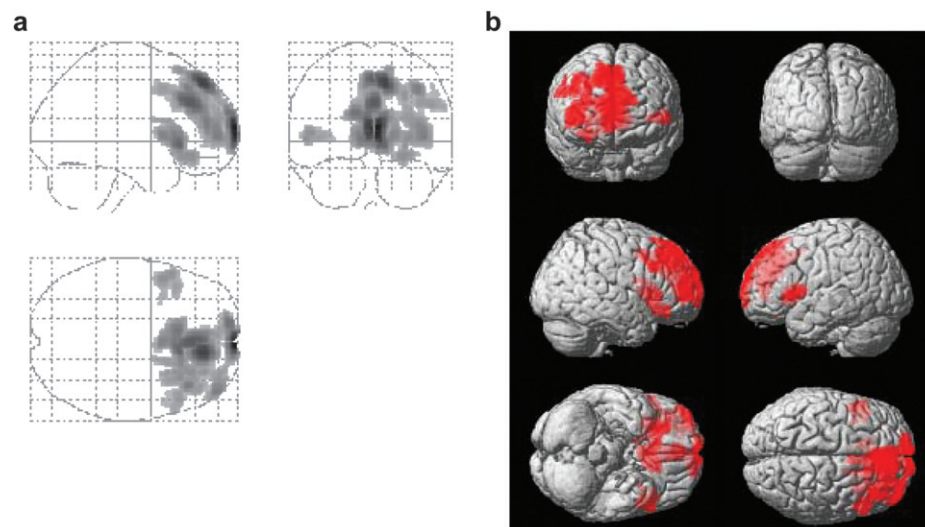

Figure 6. Results of voxel-based analysis of CBF decreases with age. The left panel (*a*) shows the glass brain overlay, and the right panel (*b*) shows the rendering on the Montreal Neurological Institute brain template. Colored voxels indicate brain regions with age-related CBF decrease ($P < 0.005$, cluster size = 200 voxels). The differences are most pronounced in the rostral half of the brain and are more prominent in the right hemisphere.
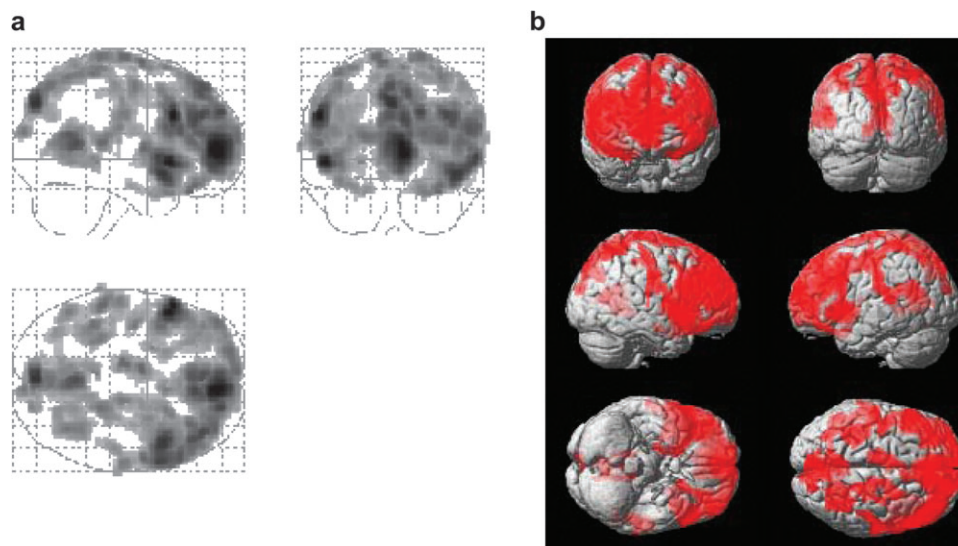

Figure 7. Results of voxel-based analysis of CVR decrease with age. The left panel (*a*) shows the glass brain overlay, and the right panel (*b*) shows the rendering on the Montreal Neurological Institute (MNI) brain template. Colored voxels indicate brain regions with age-related CVR decrease ($P < 0.005$, cluster size = 200 voxels). The CVR alterations cover the majority of the brain with the exception of occipital pole and are more prevalent than the CBF alterations.
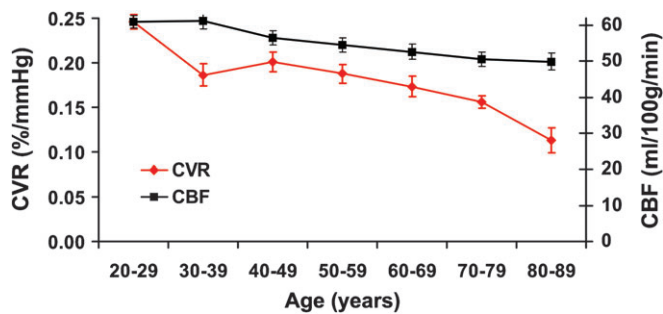
Figure 8. Decade-by-decade alterations in prefrontal CVR and CBF. Display scales for CVR and CBF are shown on the left and right axis, respectively. The display scales were set such that the first points of the 2 curves overlapped. It can be seen that CVR manifests a more rapid decay with age compared with CBF. The subjects in each decade were grouped, and the data shown are the mean and standard error of the group.

of CBF and CVR alterations in prefrontal cortex. It can be seen that CVR shows a faster decay with age. Comparing subjects in the 80s with those in the 20s, the averaged CBF decreased by 18%, whereas the CVR decreased by 54%. This observation is also consistent with the above findings that CVR decline involves a larger portion of the brain than CBF.

Gender Differences in Physiologic Parameters

Gender effects were also obtained from the regression analysis described above. It was found that female subjects had significantly higher Y_v ($P = 0.0205$), CBF ($P < 0.0001$), and CMRO$_2$ ($P < 0.0001$) compared with male subjects. The differences were 2.1%, 10.0 ml/100 g/min, and 22.0 μmol/100 g/min for Y_v, CBF, and CMRO$_2$ respectively. No gender effects were observed for CVR.

Discussion

In the present study, we conducted an investigation of age-related differences in brain metabolism and vasculature in a relatively large cohort of healthy subjects. We found that the brain's energy homeostasis is disturbed in aging due to an increase in oxygen demand and a concomitant reduction in blood supply. Such an alteration occurred early in middle age. The pattern of CBF decline is heterogeneous across the brain with prefrontal cortex, insular cortex, and caudate being the most affected regions. Aside from the age-related differences in resting state CBF, the blood vessels' ability to dilate and to dynamically adjust CBF was also reduced with age, the extent of which is more prominent than that of the resting state CBF.

To our knowledge, this work represents the most thorough investigation of metabolic and vascular physiology in aging with multiple static and dynamic parameters assessed in the same cohort. Age-related CBF differences have been extensively studied in the literature using various imaging modalities and our finding of a CBF decrease with age is in general agreement with most previous reports (Devous et al. 1986; Hagstadius and Risberg 1989; Leenders et al. 1990; Martin et al. 1991; Bertsch et al. 2009; Heo et al. 2010). A novel finding from the present study is that we observed a highly significant decrease in venous oxygenation (i.e., an increase in oxygen extraction fraction, OEF) with age. Very few studies in the literature assessed OEF in normal aging due to the need of radiotracer injection and arterial blood sampling. The few studies that measured OEF all failed to

identify a significant effect of age (Frackowiak et al. 1980; Yamaguchi et al. 1986; Leenders et al. 1990; Marchal et al. 1992), possibly because of variations in individual values and a relatively small sample size (ranging from 12–34 subjects). Owing to the recent development in noninvasive oxygenation mapping techniques (Lu and Ge 2008), we were able to measure venous oxygenation in 232 subjects, and the results unequivocally showed an age-related difference in OEF, demonstrating a disturbed balance between oxygen supply and consumption in aging. We should note that the TRUST MRI technique, by its design principle, is not susceptible to brain atrophy because the method is based on the MR T_2 decay time constant rather than on the MR signal itself (Lu and Ge 2008). Thus, the age-related reduction in tissue volume is not a confounding factor in our oxygenation measurement.

Another interesting observation was that the oxygen metabolic rate, CMRO$_2$, was found to increase with age. This is opposite to most of the reports in literature, where CMRO$_2$ was found to decrease with age (Kety 1956; Yamaguchi et al. 1986; Leenders et al. 1990; Marchal et al. 1992). We hypothesized that this discrepancy is due to brain parenchyma volume reduction that is difficult to correct in previous PET and SPECT imaging studies, which would allow CSF to be partial-volumed in the measurement and result in an underestimation in CMRO$_2$ in elderly subjects. To test this hypothesis, we re-analyzed our data by calculating CMRO$_2$ per unit volume of intracranial space (instead of per unit volume of pure tissue). The results then became consistent with the previous findings, showing a significant CMRO$_2$ decrease with age ($P = 0.008$, slope = –2.4 μmol/100 g/min per decade, see Supplementary Fig. S5 for scatter plot). Therefore, our results suggest that the age-related metabolic decline reported previously may be largely driven by a reduced brain volume in older subjects. For the brain tissue that remained, the metabolic rate is actually higher in the elderly. Such a change may reflect an age-related reduction in neuronal computational efficiency or possible leakage in membrane ion channels, which necessitates more active Na$^+$/K$^+$-ATPase pumps to maintain the membrane polarity (D'Esposito et al. 2003; Iadecola et al. 2009). For comparison, we note that a few studies have measured whole-body metabolic rate as a function of age (Krems et al. 2005; Frisard et al. 2007; St-Onge and Gallagher 2010). It was found that whole-body metabolic rate decreases with age. Much of these age-related changes can be explained by the change in body composition (i.e., more fat mass and less fat-free mass) and a reduction in physical activity (Luhrmann et al. 2009) Interestingly, after adjusting for body composition and physical activity, the remaining energy expenditure actually increased with age, a finding similar to the present study conducted for the brain.

The spatial patterns of CBF decline are comparable with those reported previously, with prefrontal cortex and insular cortex among the most affected regions (Leenders et al. 1990). A noteworthy observation is that the right prefrontal cortex showed considerably greater affected areas compared with the left hemisphere (see Fig. 6), suggesting that the right prefrontal cortex may be more vulnerable to age-related changes. This finding is interesting because there are numerous reports from the fMRI literature that the right prefrontal cortex is activated more in old compared with young adults on tasks that are typically left-lateralized in young (Cabeza et al. 1997; Gutchess et al. 2005; Duverne et al. 2009). The present data, when

combined with fMRI data, will permit a determination of the role that CBF plays in this effect and will be the subject of a later report.

The age-related alterations in CVR were found to be more prevalent than those of CBF, in terms of both the spatial extent (Fig. 7) and the percentage (Fig. 8). Therefore, it appears that age has a greater effect on the dynamic properties of cerebrovasculature compared with the static properties. Elderly individuals may have sufficient blood supply under resting conditions, but under challenge conditions such as those induced by cognitively demanding tasks, the vasculature may not be able to provide adequate blood supply, which could cause a transient ischemia to the neuronal tissue.

The findings of age-related CVR reduction also have important implications for understanding neural activity changes in aging using fMRI. FMRI is a powerful neuroimaging tool to probe neural activity via indirect effect on blood flow and blood oxygenation. There have been numerous fMRI studies in recent years to characterize changes in neural activity with age (for a review, see D'Esposito et al. 2003). With a few exceptions, most studies did not account for the effect of vascular changes on the fMRI signals. These studies have reported that neural activation was reduced with age in many brain regions but was enhanced in a few selected regions. Given our observation of a widespread decrease of CVR with age, it is possible that some of the fMRI signal reduction was simply a manifestation of vascular decline. It also suggests that the extent of enhanced neural activation with age may be more pronounced than currently thought. Such a reexamination may be particularly relevant for prefrontal cortex where our data suggest that the CVR can decrease by more than 50% comparing subjects in the 80s with those in the 20s (Fig. 8).

In the present study, we also observed a sex difference in that women had higher CBF and CMRO2 than men. This CBF difference has been reported previously by a number of investigators (Devous et al. 1986; Rodriguez et al. 1988; Bertsch et al. 2009). Several hypotheses were proposed to explain this difference. One possibility is that women have lower hematocrit levels, thus in order to carry an equal amount of oxygen, higher CBF is needed (Shaw et al. 1984). Another hypothesis states that the heart actually delivers a similar amount of blood to the brain in men and women (Baxter et al. 1987). However, since women tend to have a smaller brain volume, the CBF value per weight of brain tissue becomes greater. Another possibility for higher CBF in women is to match the higher metabolic rate as described below. The present study observed a sex-dependent CMRO2 difference with women having a higher average value. This was not noted in previous CMRO2 studies (Yamaguchi et al. 1986; Leenders et al. 1990; Marchal et al. 1992). For cerebral metabolic rate of glucose, some reports have suggested a higher value for women and attributed this difference to the influence of estrogens, which regulate basal body temperature, ionic balance, and body fluid (Baxter et al. 1987). However, other studies using similar techniques have found no apparent differences between men and women (Miura et al. 1990). Thus, the sex differences in brain energy consumption may require further investigation.

In this study, the subject recruitment criteria were based on standard protocols for brain and cognitive aging research. Individuals with neurological, psychiatric conditions, or brain tumors were excluded, and the mean MMSE score of the participants was 28.2. With this set of criteria, our data are expected to represent the normal aging effect in the general population. We did not exclude participants with genetic risk factors for dementia (e.g., APOE ε4) or those with hypertension or hypercholesterolemia because these are very prevalent risk factors in the general population, especially in older subjects. If we were to exclude these subjects, we would be effectively comparing normal young subjects to supernormal older subjects. However, these are important questions and, in our future studies, we will investigate these issues by making comparisons between age-matched normotensive and hypertensive subjects, those with and without genetic risk factors, and elderly subjects with and without amyloid depositions.

We recognize that brain volume shows an age-related decline and this effect, if not accounted for, may become a confounding factor in the comparison of metabolic and vascular parameters. Therefore, in our data analysis, we have paid special attention to minimize the partial volume effect. For the global measures, we used high resolution images ($1 \times 1 \times 1$ mm^3) to delineate pure brain parenchyma, then the metabolic and vascular parameters were calculated based on tissue volume after excluding CSF space. For the regional measures, we employed 2 separate procedures. We first used an elastic registration algorithm to match the individual brain to a brain template (Shen and Davatzikos 2002). To account for any residual brain volume effect, we included the gray matter and CSF partial volumes as covariates in the regression analysis.

The findings from the present study need to be interpreted in the context of a few limitations. The participants in this study are both healthier and somewhat more educated than the general population of older adults. We sought to recruit a healthier than average aging sample to help control unwanted noise that could confound understanding of the biological process of aging. Thus, our results should be viewed as a "best-case-scenario" model of the healthy aging brain. Several of the parameters reported in this study, specifically venous oxygenation and CMRO2, are whole-brain measures without regional information. Due to technical challenges, our MRI methods do not allow measurement of these parameters on a voxel-by-voxel basis. Therefore, it is not known whether the observed metabolic changes affect the whole brain or are region specific. Second, the effect size of our data was moderate despite a relatively large sample size (e.g., for CBF and CMRO2). One possible reason is that there were large intersubject variations even within the same age group, presumably associated with the subject's physiologic state (e.g., breathing rate and arousal level) at the time of MR acquisition. Another possible reason for the small effect size is that the effect may be region-specific and, when a global measure is taken, the effect is averaged out. Finally, our MRI techniques used a number of assumptions in estimating CBF, venous oxygenation and CMRO2, thus errors in these assumptions may be propagated to the physiologic parameters reported. However, since these assumptions are not age dependent, they would only reduce the power of the data but should not cause false positive observations.

In summary, we used noninvasive MRI techniques to assess metabolic and vascular functions across the adult life span. Age-related differences were observed in each of the physiologic parameters studied. Characterization of these basic physiologic processes may be useful for understanding the mechanisms of age-related changes in cognitive function. In addition, alterations in vascular function have strong implications for interpretation of fMRI signals in cognitive aging.

References

Andrews-Hanna JR, Snyder AZ, Vincent JL, Lustig C, Head D, Raichle ME, Buckner RL. 2007. Disruption of large-scale brain systems in advanced aging. Neuron. 56:924-935.

Ashburner J, Friston KJ. 2000. Voxel-based morphometry—the methods. Neuroimage. 11:805-821.

Aslan S, Xu F, Wang PL, Uh J, Yezhuvath U, van Osch M, Lu H. 2010. Estimation of labeling efficiency in pseudo-continuous arterial spin labeling. Magn Reson Med. 63:765-771.

Attwell D, Laughlin SB. 2001. An energy budget for signaling in the grey matter of the brain. J Cereb Blood Flow Metab. 21:1133-1145.

Baxter LR, Jr. Mazziotta JC, Phelps ME, Selin CE, Guze BH, Fairbanks L. 1987. Cerebral glucose metabolic rates in normal human females versus normal males. Psychiatry Res. 21:237-245.

Bertsch K, Hagemann D, Hermes M, Walter C, Khan R, Naumann E. 2009. Resting cerebral blood flow, attention, and aging. Brain Res. 1267:77-88.

Bohnen NI, Muller ML, Kuwabara H, Constantine GM, Studenski SA. 2009. Age-associated leukoaraiosis and cortical cholinergic deafferentation. Neurology. 72:1411-1416.

Cabeza R, Grady CL, Nyberg L, McIntosh AR, Tulving E, Kapur S, Jennings JM, Houle S, Craik FI. 1997. Age-related differences in neural activity during memory encoding and retrieval: a positron emission tomography study. J Neurosci. 17:391-400.

Cepeda NJ, Kramer AF, Gonzalez de Sather JCM. 2001. Changes in executive control across the life span: examination of task-switching performance. Dev Psychol. 37:715-730.

Craik FI. 1983. On the transfer of information from temporal to permanent memory. Philos Trans R Soc Lond B Biol Sci. 302:341-359.

Dai W, Garcia D, de Bazelaire C, Alsop DC. 2008. Continuous flow-driven inversion for arterial spin labeling using pulsed radio frequency and gradient fields. Magn Reson Med. 60:1488-1497.

D'Esposito M, Deouell LY, Gazzaley A. 2003. Alterations in the BOLD fMRI signal with ageing and disease: a challenge for neuroimaging. Nat Neurosci. 4:863-872.

Devous MD Sr, Stokely EM, Chehabi HH, Bonte FJ. 1986. Normal distribution of regional cerebral blood flow measured by dynamic single-photon emission tomography. J Cereb Blood Flow Metab. 6:95-104.

Duverne S, Motamedinia S, Rugg MD. 2009. The relationship between aging, performance, and the neural correlates of successful memory encoding. Cereb Cortex. 19:733-744.

Folstein MF, Folstein SE, McHugh PR. 1975. "Mini-mental state". A practical method for grading the cognitive state of patients for the clinician. J Psychiatr Res. 12:189-198.

Frackowiak RS, Lenzi GL, Jones T, Heather JD. 1980. Quantitative measurement of regional cerebral blood flow and oxygen metabolism in man using 15O and positron emission tomography: theory, procedure, and normal values. J Comput Assist Tomogr. 4:727-736.

Frisard MI, Broussard A, Davies SS, Roberts LJ, 2nd, Rood J, de Jonge L, Fang X, Jazwinski SM, Deutsch WA, Ravussin E. 2007. Aging, resting metabolic rate, and oxidative damage: results from the Louisiana Healthy Aging Study. J Gerontol A Biol Sci Med Sci. 62:752-759.

Garcia DM, de Bazelaire C, Alsop D. 2005. Pseudo-continuous flow driven adiabatic inversion for arterial spin labeling. Intl Soc Mag Reson Med. 13:37.

Gutchess AH, Welsh RC, Hedden T, Bangert A, Minear M, Liu LL, Park DC. 2005. Aging and the neural correlates of successful picture encoding: frontal activations compensate for decreased medial-temporal activity. J Cogn Neurosci. 17:84-96.

Guyton AC, Hall JE. 2005. Respiration. In: Guyton AC, Hall JE, editors. Textbook of medical physiology. Philadelphia (PA): Saunders, Elsevier. p. 502-512.

Hagstadius S, Risberg J. 1989. Regional cerebral blood flow characteristics and variations with age in resting normal subjects. Brain Cogn. 10:28-43.

Hasher L, Zacks RT. 1988. Working memory, comprehension and aging: A review and a new view. In: Bower GH, editor. The psychology of learning and motivation. San Diego (CA): Academic Press. p. 193-225.

Heo S, Prakash RS, Voss MW, Erickson KI, Ouyang C, Sutton BP, Kramer AF. 2010. Resting hippocampal blood flow, spatial memory and aging. Brain Res. 1315:119-127.

Herscovitch P, Raichle ME. 1985. What is the correct value for the brain–blood partition coefficient for water? J Cereb Blood Flow Metab. 5:65-69.

Iadecola C. 2004. Neurovascular regulation in the normal brain and in Alzheimer's disease. Nat Rev Neurosci. 5:347-360.

Iadecola C, Park L, Capone C. 2009. Threats to the mind: aging, amyloid, and hypertension. Stroke. 40:S40-S44.

Johnson NA, Jahng GH, Weiner MW, Miller BL, Chui HC, Jagust WJ, Gorno-Tempini ML, Schuff N. 2005. Pattern of cerebral hypoperfusion in Alzheimer disease and mild cognitive impairment measured with arterial spin-labeling MR imaging: initial experience. Radiology. 234:851-859.

Kennedy KM, Erickson KI, Rodrigue KM, Voss MW, Colcombe SJ, Kramer AF, Acker JD, Raz N. 2009. Age-related differences in regional brain volumes: a comparison of optimized voxel-based morphometry to manual volumetry. Neurobiol Aging. 30:1657-1676.

Kety SS. 1956. Human cerebral blood flow and oxygen consumption as related to aging. J Chronic Dis. 3:478-486.

Kety SS, Schmidt CF. 1948. The effects of altered arterial tensions of carbon dioxide and oxygen on cerebral blood flow and cerebral oxygen consumption of normal young men. J Clin Invest. 27:484-492.

Krems C, Luhrmann PM, Strassburg A, Hartmann B, Neuhauser-Berthold M. 2005. Lower resting metabolic rate in the elderly may not be entirely due to changes in body composition. Eur J Clin Nutr. 59:255-262.

Leenders KL, Perani D, Lammertsma AA, Heather JD, Buckingham P, Healy MJ, Gibbs JM, Wise RJ, Hatazawa J, Herold S, et al. 1990. Cerebral blood flow, blood volume and oxygen utilization. Normal values and effect of age. Brain. 113(Pt 1):27-47.

Li M, Ratcliffe SJ, Knoll F, Wu J, Ances B, Mardini W, Floyd TF. 2006. Aging: impact upon local cerebral oxygenation and blood flow with acute isovolemic hemodilution. J Neurosurg Anesthesiol. 18:125-131.

Lu H, Clingman C, Golay X, van Zijl PC. 2004. Determining the longitudinal relaxation time (T1) of blood at 3.0 Tesla. Magn Reson Med. 52:679-682.

Lu H, Ge Y. 2008. Quantitative evaluation of oxygenation in venous vessels using T2-Relaxation-Under-Spin-Tagging MRI. Magn Reson Med. 60:357-363.

Luhrmann PM, Bender R, Edelmann-Schafer B, Neuhauser-Berthold M. 2009. Longitudinal changes in energy expenditure in an elderly German population: a 12-year follow-up. Eur J Clin Nutr. 63:986-992.

Marchal G, Rioux P, Petit-Taboue MC, Sette G, Travere JM, Le Poec C, Courtheoux P, Derlon JM, Baron JC. 1992. Regional cerebral oxygen consumption, blood flow, and blood volume in healthy human aging. Arch Neurol. 49:1013-1020.

Martin AJ, Friston KJ, Colebatch JG, Frackowiak RS. 1991. Decreases in regional cerebral blood flow with normal aging. J Cereb Blood Flow Metab. 11:684–689.

Miura SA, Schapiro MB, Grady CL, Kumar A, Salerno JA, Kozachuk WE, Wagner E, Rapoport SI, Horwitz B. 1990. Effect of gender on glucose utilization rates in healthy humans: a positron emission tomography study. J Neurosci Res. 27:500–504.

Ogawa S, Tank DW, Menon R, Ellermann JM, Kim SG, Merkle H, Ugurbil K. 1992. Intrinsic signal changes accompanying sensory stimulation: functional brain mapping with magnetic resonance imaging. Proc Natl Acad Sci U S A. 89:5951–5955.

Park DC, Lautenschlager G, Hedden T, Davidson NS, Smith AD, Smith PK. 2002. Models of visuospatial and verbal memory across the adult life span. Psychol Aging. 17:299–320.

Park DC, Reuter-Lorenz P. 2009. The adaptive brain: aging and neurocognitive scaffolding. Annu Rev Psychol. 60:173–196.

Park DC, Smith AD, Lautenschlager G, Earles JL, Frieske D, Zwahr M, Gaines CL. 1996. Mediators of long-term memory performance across the life span. Psychol Aging. 11:621–637.

Raz N, Kennedy KM. 2009. A systems approach to age-related change: Neuroanatomical changes, their modifiers, and cognitive correlates. In: Jagust W, D'Esposito M, editors. Imaging the aging brain. New York: Oxford University Press. p. 43–70.

Raz N, Lindenberger U, Rodrigue KM, Kennedy KM, Head D, Williamson A, Dahle C, Gerstorf D, Acker JD. 2005. Regional brain changes in aging healthy adults: general trends, individual differences, and modifiers. Cerebral Cortex. 15:1676–1689.

Rodriguez G, Warkentin S, Risberg J, Rosadini G. 1988. Sex differences in regional cerebral blood flow. J Cereb Blood Flow Metab. 8:783–789.

Ross ED, Hansel SL, Orbelo DM, Monnot M. 2005. Relationship of leukoaraiosis to cognitive decline and cognitive aging. Cogn Behav Neurol. 18:89–97.

Rypma B, D'Esposito M. 2000. Isolating the neural mechanisms of age-related changes in human working memory. Nat Neurosci. 3:509–515.

Salat DH, Buckner RL, Snyder AZ, Greve DN, Desikan RS, Busa E, Morris JC, Dale AM, Fischl B. 2004. Thinning of the cerebral cortex in aging. Cereb Cortex. 14:721–730.

Salthouse TA. 1996. The processing-speed theory of adult age differences in cognition. Psychol Rev. 103:403–428.

Salthouse TA, Mitchell DR, Skovronek E, Babcock RL. 1989. Effects of adult age and working memory on reasoning and spatial abilities. J Exp Psychol Learn Mem Cogn. 15:507–516.

Shaw TG, Mortel KF, Meyer JS, Rogers RL, Hardenberg J, Cutaia MM. 1984. Cerebral blood flow changes in benign aging and cerebrovascular disease. Neurology. 34:855–862.

Shen D, Davatzikos C. 2002. HAMMER: hierarchical attribute matching mechanism for elastic registration. IEEE Trans Med Imaging. 21:1421–1439.

St-Onge MP, Gallagher D. 2010. Body composition changes with aging: the cause or the result of alterations in metabolic rate and macronutrient oxidation? Nutrition. 26:152–155.

Tzourio-Mazoyer N, Landeau B, Papathanassiou D, Crivello F, Etard O, Delcroix N, Mazoyer B, Joliot M. 2002. Automated anatomical labeling of activations in SPM using a macroscopic anatomical parcellation of the MNI MRI single-subject brain. Neuroimage. 15:273–289.

Wong EC. 2007. Vessel-encoded arterial spin-labeling using pseudocontinuous tagging. Magn Reson Med. 58:1086–1091.

Wu WC, Fernandez-Seara M, Detre JA, Wehrli FW, Wang J. 2007. A theoretical and experimental investigation of the tagging efficiency of pseudocontinuous arterial spin labeling. Magn Reson Med. 58:1020–1027.

Xu G, Antuono PG, Jones J, Xu Y, Wu G, Ward D, Li SJ. 2007. Perfusion fMRI detects deficits in regional CBF during memory-encoding tasks in MCI subjects. Neurology. 69:1650–1656.

Yamaguchi T, Kanno I, Uemura K, Shishido F, Inugami A, Ogawa T, Murakami M, Suzuki K. 1986. Reduction in regional cerebral metabolic rate of oxygen during human aging. Stroke. 17:1220–1228.

Yezhuvath US, Lewis-Amezcua K, Varghese R, Xiao G, Lu H. 2009. On the assessment of cerebrovascular reactivity using hypercapnia BOLD MRI. NMR Biomed. 22:779–786.

Zhao JM, Clingman CS, Narvainen MJ, Kauppinen RA, van Zijl PC. 2007. Oxygenation and hematocrit dependence of transverse relaxation rates of blood at 3T. Magn Reson Med. 58:592–597.